mathematics

MDPI

Article

Dynamics of a Model of Tumor–Immune Cell Interactions Under Chemotherapy

Rubayyi T. Alqahtani [1,*], Abdelhamid Ajbar [2] and Eman Hamed Aljebli [1]

[1] Department of Mathematics and Statistics, College of Science, Imam Mohammad Ibn Saud Islamic University (IMSIU), Riyadh 13318, Saudi Arabia
[2] Department of Chemical Engineering, College of Engineering, King Saud University, Riyadh 11421, Saudi Arabia; aajbar@ksu.edu.sa
* Correspondence: rtalqahtani@imamu.edu.sa

Abstract

This paper analyzes a mathematical model to investigate the complex interactions between tumor cells, immune cells (natural killer (NK) cells and CD8+ cytotoxic T lymphocytes (CTLs)) and chemotherapy. The primary objectives are to analyze tumor–immune interactions without and under treatment, identify critical thresholds for tumor eradication, and evaluate how chemotherapy parameters influence therapeutic outcomes. The model integrates NK cells and CTLs as effector cells, combining their dynamics linearly for simplicity. Tumor growth follows a logistic function, while immune–tumor interactions are modeled using a Hill function for fractional cell death. Stability and bifurcation analysis are employed to identify equilibria (tumor-free, high-tumor, and a novel middle steady state), bistability regimes, and critical parameter thresholds. Numerical simulations use experimentally validated parameter values from the literature. This mathematical analysis provides a framework for assessing the efficacy of chemotherapy by examining the dynamic interplay between tumor biology and treatment parameters. Our findings reveal that treatment outcomes are sensitive to the balance between the immune system's biological parameters and chemotherapy-specific factors. The model highlights scenarios where chemotherapy may fail due to bistability and identifies critical thresholds for successful tumor eradication. These insights can guide clinical decision making in dosing strategies and suggest combination therapies such as immunotherapy–chemotherapy synergies to shift the system toward favorable equilibria.

Keywords: bifurcation; bistability; cancer; chemotherapy; fractional cell kill law; tumor–immune cells

MSC: 92-10

Academic Editors: Sergei Petrovskii, Benito Chen-Charpentier, Souvik Roy and Hristo V. Kojouharov

Received: 2 May 2025
Revised: 16 June 2025
Accepted: 1 July 2025
Published: 5 July 2025

Citation: Alqahtani, R.T.; Ajbar, A.; Aljebli, E.H. Dynamics of a Model of Tumor–Immune Cell Interactions Under Chemotherapy. *Mathematics* **2025**, *13*, 2200. https://doi.org/10.3390/math13132200

1. Introduction

Cancer ranks among the foremost causes of mortality globally, with more than 8 million new diagnoses and approximately 5 million fatalities annually [1]. It is well known that the innate and adaptive immune systems respond to tumor cells by releasing specific antigens that are not present in healthy cells [2]. The immune system's reaction to tumor cells is primarily cell-mediated by natural killer (NK) cells and CD8+ cytotoxic T lymphocytes (CTLs) cells [3]. NK cells function as the foremost protective mechanism in the host body and are triggered when the activating and inhibitory receptors combine to identify the

target cells [4]. CTLs are, on the other hand, essential for recognizing and destroying tumor cells as part of adaptive immunity [5].

Researchers find mathematical modeling to be a significant asset in their efforts to understand complex regulatory mechanisms. Additionally, it can be applied to examine the mechanisms that underpin a successful immune response to tumor cells [6,7]. Different modeling approaches have been used in the literature depending on the number of immune cells considered (NK, CD8+T, CD4+T, etc.) and the desired rigor (distributed parameter models or PDEs, lumped parameter models or ODEs, stochastic models and models with time delay) [8–19].

In this regard, the model presented by Kuznetsov et al. [8] was one of the earliest and basic ODE models used to depict the interactions between immune cells and cancer as a predator–prey relationship. The model comprised two classes of cells, one representing the population of effector cells (the predator) and the other representing the population of tumor cells (the prey). The model analysis [8] identified regions of bistability, parameter spaces where only one class of cells exists, and areas where dormant tumor cells can sneak in immune surveillance and become active. The system in [8] was further modified by Bashkirtseva et al. [17] by adding the chemotherapy treatment. In their investigation of the impact of chemotherapy drugs, the authors [17] demonstrated the presence of regions of periodic behavior in addition to static regimes.

The model suggested in [8] and studied further in [9,17], for instance, was based on the assumption that the rate of tumor lysis or fractional cell killing (a mathematical expression that describes the rate at which a specific population of cells is reduced to a fraction of itself) would rise in a linear fashion corresponding to the number of immune cells present, much like a typical Lotka–Volterra model [20]. However, subsequent research revealed that the lysis curves seen in certain experimental settings [21,22] demonstrated saturation as the initial effector-to-target ratios increased. In order to model these experimental findings, a novel fractional cell killing expression for CD8+ lymphocytes was proposed in [10]. The foundation of this fractional cell kill law is a Hill function [23]. Based on that work, López et al. [13] developed—using the experimental work in [21]—a validated ODE model that illustrated tumor progression through the interaction of three cell populations: neoplastic tissue, healthy tissue, and immune cells. Later, Makhlouf et al. [14] studied the stability of an ODE model that forecasted the interaction between tumor cells, circulating lymphocytes, CD4+T cells, CD8+T cells, and natural killer cells without or under chemotherapy. Song et al. [15] proposed and studied the stability of a model that described the relationships between immune cells and tumors, highlighting the role of NK cells and CTLs in immune surveillance.

This paper presents a new contribution to the aforementioned studies on interactions between immune and tumor cells. We propose and analyze a model that encapsulates the key components of the interactions and makes it possible to easily visualize their dynamical behavior. In accordance with research in [13], we assume that there is a linear relationship between the growth dynamics of the two immune populations, NK and CTLs cells. In this way, we simply refer to both cells as effector cells and linearly combine their equations. The novelty of this study lies in two aspects: (1) the proposed model includes growth rates that were overlooked in previous models [13], and (2) the numerical analysis is carried out using bifurcation analysis, which allows for the construction of practical branch sets that determine the regions of bistability, facilitate the evaluation of the effect of model parameters on interactions, and are used to investigate the impact of the intensity of chemotherapy drug on treatment outcomes.

The remainder of this paper is structured as follows: Section 2 presents the model, and Section 3 examines the stability of tumor-free equilibrium. Section 4 discusses the choice

of model parameters. Section 5 examines the model without chemotherapy. Section 6 examines the model with chemotherapy, and the final section includes a discussion and concluding remarks.

2. The Mathematical Model

In the model presented in this work, two immune cell populations—natural killers (NK) and CD8+ T lymphocytes (cytotoxic T lymphocytes, or CTLs)—interact with a tumor cell population T. Similarities exist between the growth of NK and CTL cells. Three terms are involved in the growth of both cells: one for recruitment, one for competition with tumor cells, and one for death. The two cells' growth dynamics differ noticeably in that NK cells have a constant input for innate immunity, whereas CTL cells do not as they are associated with acquired immunity. The dynamics of CTLs also include the stimulation of T lymphocy in light of the interaction occurring between NK cells and cancerous cells in addition to an activation term.

In this paper, we assume that the growth dynamics of the two immune cell populations (NKs and CTLs) are linearly related in accordance with the work in [13]. Hence, we simply refer to them as effector cells E and linearly combine their equations. As a result, there are two classes of cells in the model: Class T, which represents the tumor cell (prey) population, and Class E, which represents the effector cell (predator) population. The model equations are as follows:

$$\frac{dT}{dt} = \alpha T(1-\beta T) - \gamma ET - \nu D(E,T)T - k_1 CT \tag{1}$$

$$\frac{dE}{dt} = \sigma - \delta E + \frac{jT^2E}{k+T^2} + \frac{gD^2T^2E}{h+D^2T^2} - \phi ET - k_2 CE \tag{2}$$

$$\frac{dC}{dt} = -\mu C + u. \tag{3}$$

E (cell) and T (cell) denote concentrations of effector cells and tumor cells, respectively. The growth of tumor cells T is assumed to follow a logistic law with growth rate α (1/day) and a carrying capacity $\frac{1}{\beta_1}$ (1/cell). Tumor cell reduction owing to effector cells is represented by γET, where the rate of tumor cell lysis is denoted by γ (1/cell·day). Additionally, tumor cells are destroyed by chemotherapy at a rate of k_1 (m^2/mg·day). The term $D(E,T)$ represents the fractional tumor cell killing by T cells. It is given by a Hill function [10–23] that depends on the ratio of E/T, giving rise to the de Pillis–Radunskaya–Wiseman (PRW) law [10]:

$$D(E,T) = \frac{(E/T)^\tau}{s + E/T^\tau} = \frac{E^\tau}{sT^\tau + E^\tau} \tag{4}$$

The parameter τ is related to the tumor's geometry. Tumors exhibiting reduced sphericity are linked to higher τ values. On the other hand, the parameter s is indicative of the innate proficiency of cytotoxic cells in recognizing and destroying their targets. Smaller s values are associated with more effective immune cell responses [10].

It should be noted that the Hill function [23] is often used in mathematical models of biological systems, including tumor–immune interactions, to describe saturation effects (e.g., immune cell activation or suppression). In the context of tumor–immune dynamics, it can model how immune responses depend on tumor cell numbers. One general form of the Hill function is $H = \frac{x^n}{K^n + x^n}$ where x is the input (e.g., tumor cell population, cytokine concentration), n is the steepness, and K is a saturation constant.

For effector cells, the population (Equation (2)) increases at a constant rate of σ (cell/day) responsible for innate immunity, and it decreases at a constant rate of δ (1/day) in a natural demise. The decrease in effector cells is also due to their interactions with

tumor cells ϕET at a rate of ϕ (1/cell·day). Additionally, effector cells are destroyed by chemotherapy at a rate of k_2 (m^2/mg·day).

The dynamics of effector cells includes two recruitment terms: the first one corresponds to a simple power law $\frac{jT^2E}{(k+T^2)}$, where j (1/day) is the maximum recruitment rate and k (cells^2) is the steepness coefficient for the recruitment. This recruitment term is predominately associated with NK cells [13]. The second term is represented by the PRW law [10] $\frac{gD^2T^2E}{(h+D^2T^2)}$, where g (1/day) is the maximum activation rate and h (cells^2/day^2) is the steepness coefficient of the activation [10,13]. This term is predominately associated with CTL cells [10,13]. These two terms are now described as functions of the effector cells E, as the two types of immune cells are lumped.

The third equation (Equation (3)) represents the change in the concentration of the chemotherapy drug over time at a rate μ (1/day). The term u (mg/BSA·day) represents the daily dose of the chemotherapy drug, where BSA (m^2) indicates the body surface area. The BSA method is often used in chemotherapy treatments for cancer, where the dosage needs to be carefully tailored to the patient's body size; it is more accurate than than weight-based methods. As a result, the fractional cell kill parameters k_1 and k_2 have a dimension of (m^2/mg·day). The simplification used in this paper to lump natural killer (NK) cells and CD8+ T cells into a single "effector cell" population is supported by experimental and theoretical evidence but also has limitations depending on the research context. We present in the following an examination of when and why this simplification is appropriate. The first issue has to do with the functional overlap in tumor killing. Both NK cells and CD8+ T cells contribute to tumor cell lysis through similar mechanisms, including perforin/granzyme [24] and Fas-FasL [25], suggesting that their combined effect can be approximated in a single population when modeling total cytotoxic pressure.

The second issue has to do with synergistic effects in immunotherapy: some immunotherapies activate both NK and CD8+ T cells through shared pathways, justifying a unified "cytotoxic response" in models. Waldhauer and Steinle [26] showed that NKG2D ligands on tumors activate both NK and CD8+ T cells similarly. Galon and Bruni [27] discussed how the concept of "Immunoscore" in cancer often combines CD8+ T and NK cell densities as a prognostic marker because both correlate with survival. This implies that from a clinical outcome perspective, the combination of their effects is meaningful. As result of these considerations, several mathematical models use a single effector equation when differences between NK and CD8+ T cells are not critical [8,9,17,28]. The experimental work of Diefenbach et al. [21] confirmed that NK and CD8+ T cells often cooperate in tumor suppression, supporting the idea of combined cytotoxic potential. Eftimie et al. [29] reviewed tumor–immune models and noted simplifications when studying tumor escape mechanisms rather than immune subtypes. De Pillis et al. [10] combined effectors when modeling chemotherapy effects, arguing that net tumor killing matters more than individual contributions. López et al. [13] demonstrated additive contributions of NK and CD8+ T cells in early tumor control and suggested that if the focus is on total tumor lysis rather than subtype dynamics, lumping is reasonable.

Lumping the two cells has, on the other hand, some limitations. One issue concerns the differences in response time: NK cells respond within hours/days, while CD8+ T cells require days/weeks [30]. There is also the issue of therapy specificity: checkpoint inhibitors (e.g., anti-PD-1) primarily target CD8+ T cells and not NK cells [31]. The two immune cells also have distinct suppression mechanisms; tumors may evade NK cells (e.g., MHC-I downregulation) but suppress CD8+ T cells via PD-L1 [32].

In conclusion, lumping NK and CD8+ T cells is a practical simplification for models prioritizing overall tumor–immune dynamics, such as the one presented in this paper, where the focus is on net tumor killing. However, separate modeling is essential for studies

requiring mechanistic precision, such as those studying immunotherapies targeting only one subset (e.g., CAR-T cells), if timescales of NK vs. CD8+ T cell responses are critical, or if it is necessary to model immune evasion strategies that are specific to each cell type.

The model is made dimensionless by employing the following variables:

$$\bar{T} = \beta T, \bar{E} = \frac{\alpha E}{\sigma}, \bar{C} = \frac{C}{C_0}, \bar{t} = \alpha t, \bar{\gamma} = \frac{\gamma\sigma}{\alpha^2}, \bar{\nu} = \frac{\nu}{\alpha}, \bar{k}_1 = \frac{k_1 C_0}{\alpha}, \bar{\delta} = \frac{\delta}{\alpha}$$
$$\bar{j} = \frac{j}{\alpha}, \bar{g} = \frac{g}{\alpha}, \bar{k} = k\beta^2, \bar{h} = \beta^2 h, \bar{\phi} = \frac{\phi}{\alpha\beta}, \bar{k}_2 = \frac{k_2 C_0}{\alpha}, \bar{\mu} = \frac{\mu}{\alpha}, \bar{u} = \frac{u}{\alpha C_0}, \bar{s} = s(\frac{\alpha}{\beta\sigma})^{\tau}.$$

The dimensionless model becomes

$$\frac{d\bar{T}}{d\bar{t}} = \bar{T}(1-\bar{T}) - \bar{\gamma}\bar{E}\bar{T} - \bar{\nu}\bar{D}\bar{T} - \bar{k}_1\bar{C}\bar{T} \tag{5}$$
$$\frac{d\bar{E}}{d\bar{t}} = 1 - \bar{\delta}E + \frac{\bar{j}\bar{T}^2\bar{E}}{\bar{k}+\bar{T}^2} + \frac{\bar{g}\bar{D}^2\bar{T}^2\bar{E}}{\bar{h}+\bar{D}^2\bar{T}^2} - \bar{\phi}\bar{E}\bar{T} - \bar{k}_2\bar{C}\bar{E} \tag{6}$$
$$\frac{d\bar{C}}{d\bar{t}} = -\bar{\mu}\bar{C} + \bar{u} \tag{7}$$
$$\bar{D} = \frac{\bar{E}^{\tau}}{\bar{s}\bar{T}^{\tau} + \bar{E}^{\tau}} \tag{8}$$

It can be noted that the model variables are rendered dimensionless by utilizing solely (α (1/day), β (1/cell)), which represent the parameters of the logistic growth rate, the growth rate of effector cells σ (cell/day), and a reference value for drug concentration C_0 (mg/m^2). It is known that the values of tumor growth rates α and β depend not only on the type of tumors but also on their stages of development. Consequently, the examination of the dimensionless model through variations of its dimensionless parameters around certain experimentally validated values constitutes a useful study that can be correlated with various tumor cases and stages. Conversely, the reference drug concentration C_0 solely influences the dimensionless values of chemotherapy drug dose $\bar{u}$ and values of fractional cell kill parameters $\bar{k}_1$ and $\bar{k}_2$.

In the rest of this manuscript, we drop the *bar* notation from all variables and parameters.

3. Equilibria Existence and Classification

In the following analysis, we examine the presence of real and positive equilibria within the framework of the model defined by Equations (5)–(8). Equation (7) at steady-state yields $C = \frac{u}{\mu}$. Substituting the expression of D (Equation (8)) into Equations (5) and (6) yields the following two equations as a function of E and T:

$$ln\frac{E^{\tau}}{sT^{\tau}+E^{\tau}} = \frac{1-\gamma E - k_1 CT}{\nu}. \tag{9}$$

$$a_3E^3 + a_2E^2 + a_1E + a_0 = 0, \tag{10}$$

where the coefficients $(a_i, i = 1, 3)$ depend explicitly on T and are shown in Appendix A. Note that Equation (9) is transcendental and can only be solved numerically. We can deduce from Equations (9) and (10) that the maximum number of equilibria (other than the tumor-free one) is three. Details of this result and the stability of the non-trivial equilibrium are shown in Appendix A. However, because of the transcendental nature of the equations, any analysis of stability or saddle–node bifurcation can only be carried out numerically.

The model tumor-free equilibrium is $(T = 0, E = \frac{1}{\delta + k_2 \frac{u}{\mu}})$. The eigenvalues of the Jacobian matrix in this steady state (with details given in Appendix B) are $\lambda_1 = -\mu, \lambda_2 = -\delta - \frac{k_2 u}{\mu}$, while the third eigenvalue satisfies the following quadratic equation:

$$a\lambda^2 + b\lambda + c = 0, \tag{11}$$

with

$$a = -k_1 k_2, b = \mu((1-\nu)k_2 - \delta k_1), c = \mu^2((1-\nu)\delta - \gamma). \tag{12}$$

4. Model Baseline Parameters

In conducting numerical simulations, the values of the model parameters shown in Table 1 were carefully chosen to align with realistic situations. The model parameters were validated under two conditions: without treatment and during chemotherapy, as detailed in [13]. In the untreated scenario, validation was achieved by replicating immune-mediated tumor lysis, supported by experimental data fitting, dynamical analysis, and residual comparisons to ensure biological plausibility. Growth curves in the absence of an immune response, derived from data in [21], facilitated the estimation of tumor logistic growth parameters α and β. These parameters were determined by minimizing the least-squares distance between simulated values and experimental data. Additionally, immune recruitment rates were approximated using measurements of IFN-γ (Interferon gamma), producing immune cells as a function of ligand expression, comparing ligand-transduced and control-transduced tumor cells. The background source rate for immune cells σ and their death rate d were sourced from experiments reported in [8]. Parameters governing tumor–immune interactions, such as the fractional kill rate γ, immune recruitment coefficients (j, k, g, h), and competition term ϕ were adopted from prior validated models [10], ensuring alignment with established tumor biology. The fractional kill function $D(E, T)$ (Equation (4)) was calibrated against experimental lysis data [21], which examined tumor rejection mediated by NK cells and CD8+ T cells in mice. Least-squares fitting was employed to adjust $D(E, T)$ parameters, matching experimental effector-to-target (E–T) cytotoxicity curves across various immune challenges.

For the chemotherapy model, an exponential kill model $k(1 - \exp^{-\rho C(t-\tau)})$ was used in [13], with parameters reflecting drug pharmacodynamics. The drug resistance coefficient ρ and time delay (τ) were fitted to tumor regression data [13], where mice with plasmacytomas were treated with cyclophosphamide, and tumor regression was monitored post-treatment.

In this work, a simplified linear cell kill law (i.e., $k_1 C$, Equation (1)) was adopted, omitting drug delay and resistance effects. While this approach streamlined our mathematical analysis, it has inherent limitations. The selection of either an exponential fractional kill law or a linear cell kill law hinges on the drug's mechanism, pharmacokinetics, and the timescales under consideration. Neglecting delay effects—such as cell cycle arrest or drug uptake time—is justified when the drug action timescale is significantly shorter than the tumor growth dynamics. Similarly, disregarding resistance is valid for short-term treatments or scenarios where resistance mutations are infrequent, such as during early therapy phases.

Table 1. Model baseline parameters [10,13,21].

Parameter	Definition	Value	Unit	Dimensionless Value
C_0	Reference value for concentration of chemotherapy drug	10^3	$mg.m^{-2}$	-
g	Maximum recruitment rate related to the PRW law	0.0375	day^{-1}	0.073
h	Steepness coefficient for recruitment related to the PRW law	2.02×10^7	$cell^2$	1.75×10^{-12}
j	Maximum recruitment rate related to the power law	0.0357	day^{-1}	0.073
k	Steepness coefficient for recruitment related to the power law	2.02×10^7	$cell^2$	2.1×10^{-11}
k_1	Fractional tumor cell kill by chemotherapy	2.41	$m^2mg^{-1}day^{-1}$	4680
k_2	Fractional immune cell kill by chemotherapy	4.03	$m^2mg^{-1}day^{-1}$	7840
s	Steepness coefficient of the PRW law	2.5	-	15.9
α	Tumor cell growth rate	0.514	day^{-1}	-
β	Inverse of tumor-carrying capacity	1.0204×10^{-9}	$cell^{-1}$	-
δ	Death rate of effector cells	0.0612	day^{-1}	0.119
γ	Rate of tumor cell lysis	1.1×10^{-10}	$cell^{-1}day^{-1}$	3.12×10^{-5}
ϕ	Effector cell inactivation rate by tumor cells	2.8×10^{-9}	day^{-1}	5.34
μ	Rate of chemotherapy drug decay	0.9	day^{-1}	1.75
ν	Saturation level of fractional tumor cell kill	3.47	day^{-1}	6.75
σ	Growth rate of effector cells	7.5×10^4	$cell{\cdot}day^{-1}$	-
τ	Exponent of the PRW law	0.21	-	0.21

5. Analysis of the Model Without Chemotherapy

When the chemotherapy is not administrated, the model tumor-free equilibrium is $(T = 0, E = \frac{1}{\delta})$. The eigenvalues λ_i of the Jacobian matrix at this equilibrium are (Appendix B)

$$\lambda_1 = -\delta, \text{ and } \frac{\delta(1-\nu)-\gamma}{\delta}. \tag{13}$$

Therefore, for $\nu > 1$, the second eigenvalue is always negative, and the tumor-free equilibrium is always stable. For $\nu < 1$, the tumor-free solution is unstable for $\gamma < \delta(1-\nu)$.

For parameter values in Table 1, with $\gamma = 0.2$ for example, we can numerically solve the model equations and show that there are two steady states in addition to the tumor-free solution. The steady states are $A\ (T = 0, E = 8.4033), B\ (T = 0.1570, E = 1.2323)$ and $C\ (T = 0.5778, E = 0.3261)$. (A) is the tumor-free solution, and (B) is a saddle point characterized by low-tumor-concentration cells. Steady state (C) is a stable node and is characterized by a high tumor cell concentration and low effector cell levels, which correspond to uncontrolled tumor growth. The phase portrait is shown in Figure 1. The stable manifold of the steady state B acts as a boundary that divides the basins of attraction of (A) and (C). Initial conditions (i) and (ii) depicted in Figure 1 reside within the basin of attraction of the tumor-free equilibrium, ultimately converging towards point (A). In contrast, the initial conditions (iii) and (iv) fall within the basin of attraction of the high-tumor equilibrium. These initial conditions escape immune surveillance, leading the system

towards the high-tumor equilibrium (C). The disease's outcome is therefore significantly influenced by the basin boundary's location.

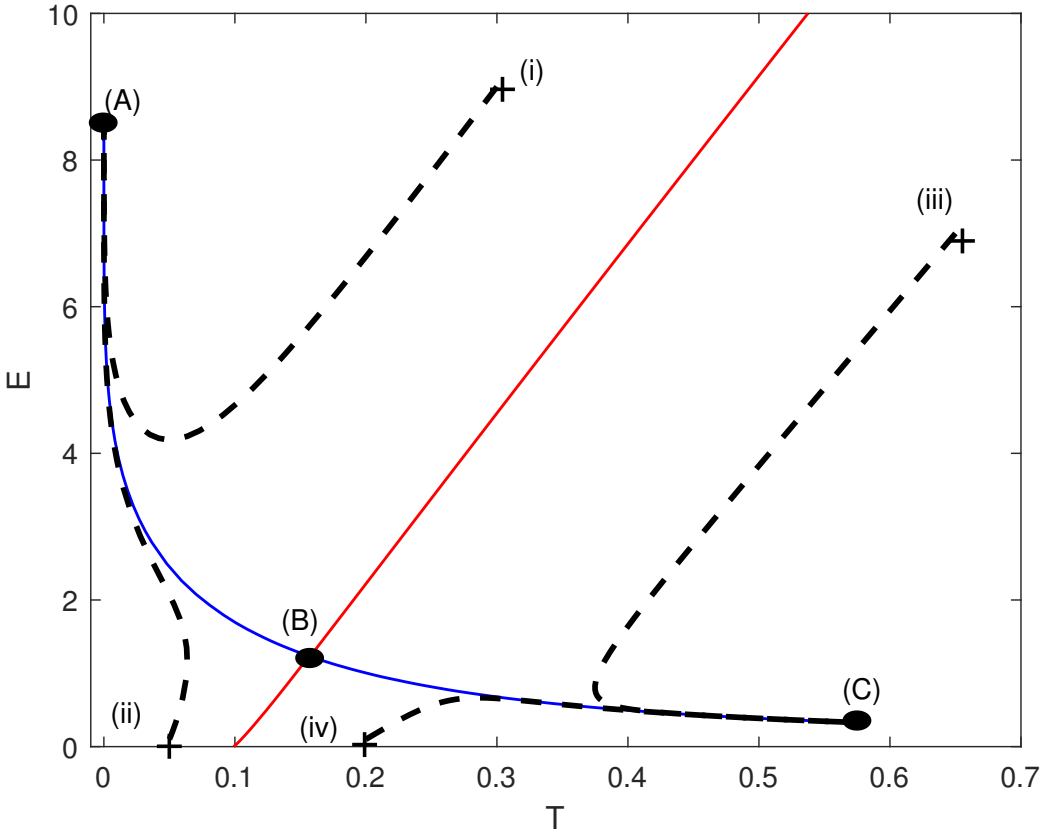

Figure 1. Phase portrait of the model (Equations (5)–(8)) with no chemotherapy at the dimensionless parameter values in Table 1 with $\gamma = 0.2$. (A) is the free-tumor equilibrium, (B) the low-tumor equilibrium, and (C) the high-tumor equilibrium. Stable manifold of saddle point B (blue); unstable manifold of saddle point B (red); initial conditions (+) for transients (dotted curves) denoted (i–iv). Initial conditions for (i) (E,T) = (0.3,9); (ii) (E,T) = (0.05,0.1); (iii) (E,T) = (0.65,7.0); (iv) (E,T) = (0.2,0.1).

By conducting a bifurcation analysis, we can better comprehend the system's overall dynamics. This kind of analysis can also identify model parameter values that act as thresholds, above which the patient's system moves into a stable tumor-free equilibrium. All bifurcation diagrams were generated using Matcont [33], a graphical MATLAB [34] software package for the bifurcation study of continuous and discrete dynamical systems.

We choose the parameter γ as the bifurcation parameter. This parameter basically describes the rate at which tumor cells are attacked due to interaction with the tumor i.e., the cytolytic potential of the immune cells. Using the model parameter's values in Table 1, Figure 2 shows that the model predicts a simple saddle–node bifurcation where a limit point is seen to occur at $\gamma = 0.3975$. Since the tumor-free equilibrium in this case is always stable (since $\nu = 6.75 > 1$), the following regimes are observed. For $0 < \gamma < 0.3975$, the system exhibits a coexistence between the tumor-free and the uncontrolled tumor equilibria. Bistability indicates that external influences on the immune system, which may intuitively be perceived as beneficial for enhancing the immune response (such as immunostimulation or modifications to initial conditions), can in reality have adverse effects. Beyond the limit point, the system's solutions stabilize at the equilibrium without tumors.

Another behavior predicted by the model is found when the tumor-free steady state is unstable. Figure 3 presents an illustration of a bifurcation diagram for $\nu = 0.5 < 1$ (Equation (13)). It can be seen that the tumor-free steady state is unstable for very small values of γ, and there is a stable high-tumor equilibrium. This corresponds to a system that

demonstrates a severely inadequate innate immune response to cancer. With an increase in the parameter γ, the stability of the tumor-free equilibrium is achieved, and there is coexistence with the stable high-tumor steady state. Once the tumor-free equilibrium reaches stability, a saddle equilibrium emerges, acting as a boundary between the two stable equilibria. The system is presently in a bistable condition, and the treatment's goal should be to position the system within the basin of attraction of the zero-tumor equilibrium. Beyond the saddle–node bifurcation, the system maintains a stable equilibrium devoid of tumors, ensuring that the disease does not advance.

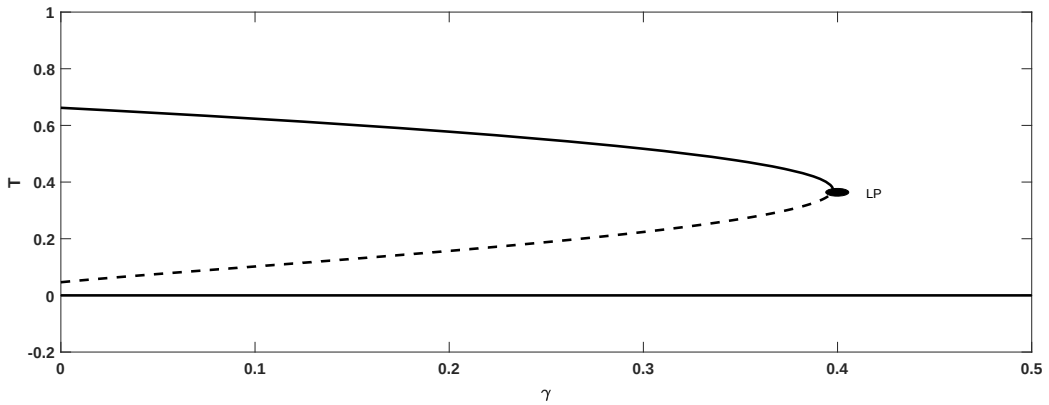

Figure 2. Bifurcation diagram for a model without chemotherapy for the system parameters in Table 1, and rate of tumor cell lysis γ as the bifurcation parameter. Solid line (stable branch), dashed line (unstable branch), LP(static limit point).

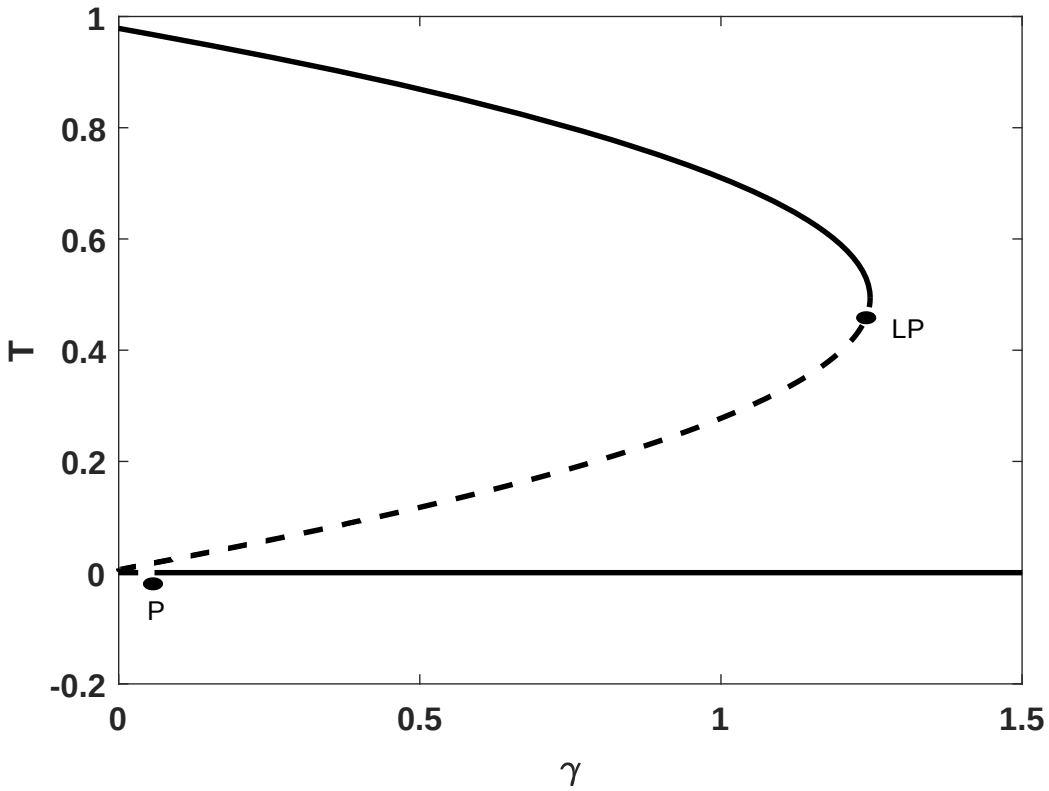

Figure 3. Bifurcation diagram for model without chemotherapy for the system parameters in Table 1 with $\nu = 0.5$ and the rate of tumor cell lysis γ as the bifurcation parameter. Solid line (stable branch); dashed line (unstable branch); LP (static limit point). (P) indicates the point of transition from unstable to stable tumor-free equilibrium.

It should be noted that the location of the point of transition (P, Figure 3) depends solely on γ, δ and ν (Equation (13)). Large values of δ or smaller values of ν would push the point (P) to occur at larger values of γ. Consequently, if the tumor-free equilibrium is unstable, any treatment must alter the system's parameters in addition to reducing the tumor burden.

Furthermore, we can map out the different regions of behavior in Figures 2 and 3 as a function of model parameters. Figure 4 shows the locus of the limit point. The effect of ν, ϕ, s and δ shows an increasing trend with γ. This means that any increase/decrease in any of these parameters as a result of some non-chemotherapy treatment will enlarge/decrease the range of bistability in terms of γ. The effect of both ν and ϕ can be seen to be linear, while the bistability region grows much faster with an increase in the parameter s. The effect of δ (shown in Figure 4d) is noticeable only when γ exceeds a certain value and the region of bistability increases almost linearly with the increase in δ. The effects of j (Figure 4e) (and g, not shown in the figure) show a decreasing trend. The increase in these activation terms reduces almost linearly in the range of the bistablity region. The effect of k (Figure 4f) (and h, not shown in the figure), shows that these parameters do not significantly affect the locus of the limit point and therefore do not alter the region of bistability much.

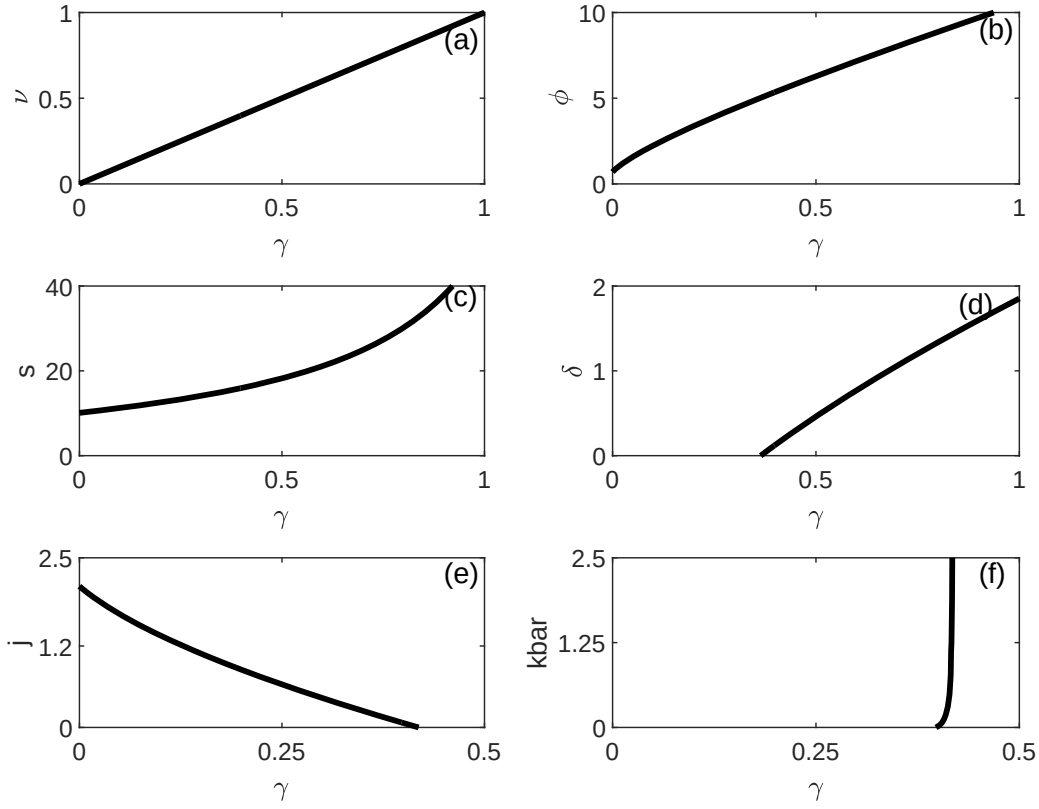

Figure 4. Two parameter continuation diagrams showing the locus of the limit point of Figure 2. (**a**) Effect of saturation level of fractional tumor cell kill ν; (**b**) effect of effector cell inactivation rate by tumor cells ϕ; (**c**) effect of steepness coefficient of the PRW law s; (**d**) effect of death rate of effector cells δ; (**e**) effect of maximum recruitment rate related to the power law j; (**f**) effect of steepness coefficient for recruitment related to the power law k.

6. Analysis of the Model with Chemotherapy

When the system is under chemotherapy, the model tumor-free steady state has two negative eigenvalues, while for the third eigenvalue, the following cases are possible for the quadratic equation (Equations (11) and (12)). A summary of the the analysis is also shown in Table 2.

1. $\nu \geq 1$. In this case, c and b are both negative, and since a, (Equation (12)) is always negative, the discriminate $\Delta = b^2 - 4ac$ can be either positive or negative. When it is positive, the product of both roots is positive, and their sum is negative, so there is no positive solution to Equation (11), and the tumor-free equilibrium is stable for all u.
2. $\nu < 1$, $c > 0$ and $b > 0$, which is equivalent to $\nu < 1$, $\nu < 1 - \frac{\gamma}{\delta}$ and $\nu < 1 - \delta\frac{k_1}{k_2}$. In this case, the discriminate is always positive, and there is only one positive solution u_1. The tumor-free equilibrium is stable for all $u > u_1$.
3. $\nu < 1$, and $c > 0$, $b < 0$, which is equivalent to $\nu < 1$, $\nu < 1 - \frac{\gamma}{\delta}$ and $\nu > 1 - \delta\frac{k_1}{k_2}$. In this case, the discriminate is always positive, and there is also only one positive solution u_1. The steady state is stable for all $u > u_1$.
4. $\nu < 1$, $c < 0$ and $b > 0$, which is equivalent to $\nu < 1$, $\nu > 1 - \frac{\gamma}{\delta}$ and $\nu < 1 - \delta\frac{k_1}{k_2}$. In this case, the discriminate can be either be positive or negative. When it is positive, there are two positive solutions u_1 and u_2, and the tumor-free equilibrium is unstable for $u_1 < u < u_2$.
5. $\nu < 1$, $c < 0$ and $b < 0$. This is equivalent to $\nu < 1$, $\nu > 1 - \frac{\gamma}{\delta}$ and $\nu > 1 - \delta\frac{k_1}{k_2}$. In this case, the discriminate can be either positive or negative, but even in the former case, there is no positive solution, and the point is stable for all values of u.

Table 2. Stability conditions for tumor-free equilibrium under chemotherapy.

Case No.	Sign of $(\nu - 1)$	Sign of (b)	Sign of (c)	Sign of $(\Delta = b^2 - 4ac)$	Number of Positive Solutions of Equation (11) If $\Delta > 0$	Stability of Trivial Equilibrium
1	+	−	−	±	0	always stable
2	−	+	+	+	1 (u_1)	stable for $u > u_1$
3	−	−	+	+	1 (u_1)	stable for $u > u_1$
4	−	+	−	±	2 (u_1, u_2)	unstable for $u_1 < u < u_2$
5	−	−	−	±	0	always stable

Following this analysis, we can distinguish between three qualitatively different bifurcation diagrams. It is more convenient to choose the chemotherapy dosage intensity (u) as the bifurcation parameter.

The first situation corresponds to $\nu > 1$. The tumor-free equilibrium point is stable for all values of u, as shown in the bifurcation diagram of Figure 5, for example, for $\nu = 6.75$, $k_1 = 4680$, and $k_2 = 7840$ and the rest of the model parameters of Table 1. The diagram is characterized by the presence of a static limit point. When the chemotherapy drug intensity (u) is larger than the limit point, the tumor cells disappear. For a drug dose below the limit point, there exits a bistability between the tumor-free equilibrium and the high-tumor cells. Again, this shows that sudden changes in system parameters and/or initial conditions may be detrimental even to the effect of the chemotherapy treatment.

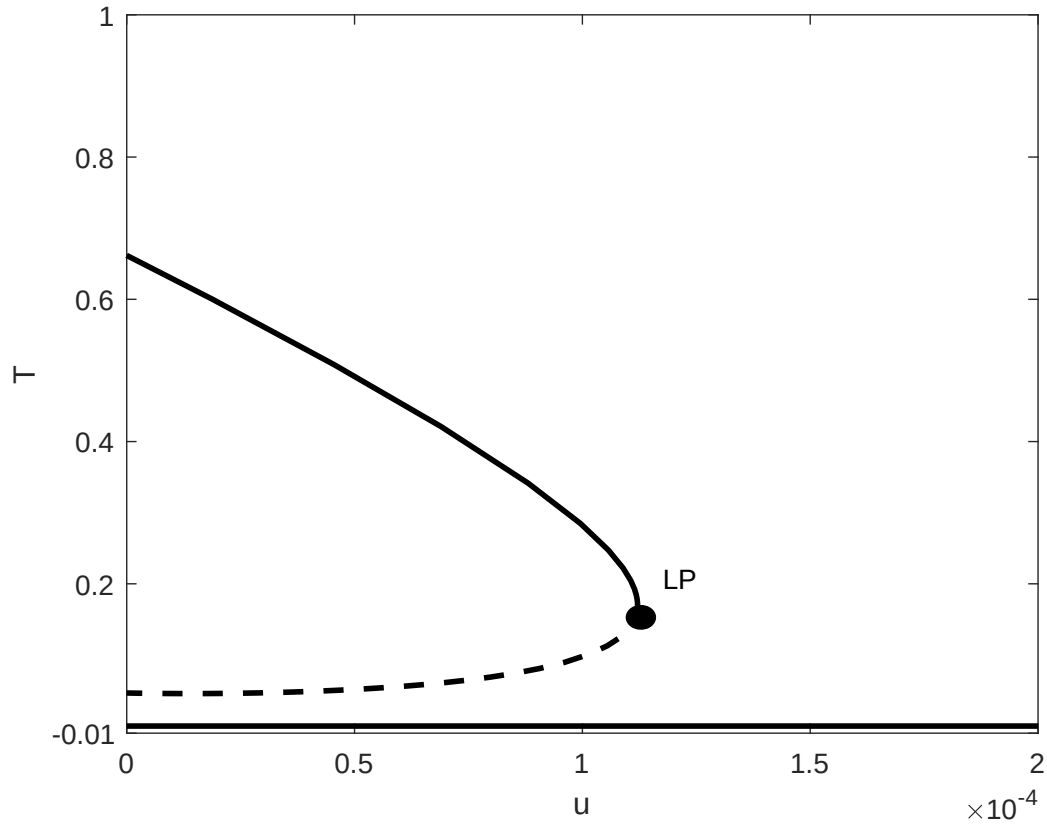

Figure 5. Bifurcation diagram for model with chemotherapy for the system parameters in Table 1, with $\nu = 6.75$ and drug intensity u as the main bifurcation parameter. Solid line (stable branch); dashed line (unstable branch); LP (static limit point).

The second situation is when the tumor-free equilibrium is unstable below a critical level of drug intensity. This situation is shown in Figure 6, for example, for $\nu = 0.9$. In this case, the tumor-free steady state is unstable for u below point P in Figure 6. This situation indicates that any level of drug intensity below the critical value is unable to suppress the tumor, and the system settles on a high tumor concentration. A coexistence between the tumor-free and high-tumor cells exists for drug intensity between the critical value and the limit point. Only values of drug intensity larger than the limit point completely suppress the tumor.

The third situation is when the tumor-free equilibrium is unstable between two critical values of u. This situation is shown in Figure 7, for example, for $\delta = 0.0005$ and $\nu = 0.97$. Figure 7a shows only the nontrivial steady state. Only values of u larger than the limit point completely destroy the tumor cells. However, Figure 7b shows the enlargement of the small rectangle close to the zero axis of Figure 7a. Two critical points (P_1) and (P_2) appear at $u_1 = 1.231 \times 10^{-7}$ and $u_2 = 1.098 \times 10^{-5}$ on the tumor-free equilibrium (red line). Moreover, there is the appearance of a middle tumor concentration branch (blue curve). For values of drug intensity smaller than P_1, the tumor-free equilibrium is stable, the middle curve is unstable, and the upper curve (Figure 7a) is stable. Consequently, there is bistability between the disease-free equilibrium and the high-tumor cell steady state. For drug intensity between P_1 and P_2, the tumor-free curve is unstable, the middle curve is stable, and the upper curve (Figure 7a) is also stable. Therefore, there is bistability where the system can settle on the middle tumor level concentration or on the high-tumor level equilibrium. For drug intensity larger than P_2 and up to the limit point, the tumor-free equilibrium is stable, the middle steady state is unstable, and the high-tumor steady state

(Figure 7a) is stable. Therefore, there is again a bistablity regime between the tumor-free equilibrium and the high-level tumor concentration.

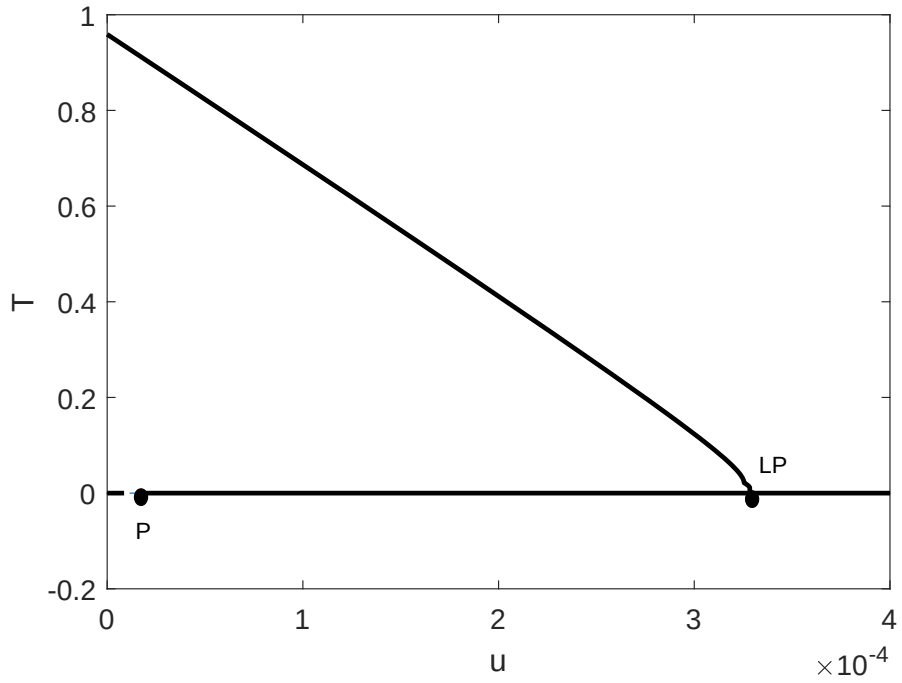

Figure 6. Bifurcation diagram for the model with chemotherapy for the system parameters in Table 1 with $\nu = 0.95$ and drug intensity u as the main bifurcation parameter. Solid line (stable branch); dashed line (unstable branch); LP (static limit point). (P) indicates the point of transition from unstable to stable tumor-free equilibrium(unstable branch, below point P) .

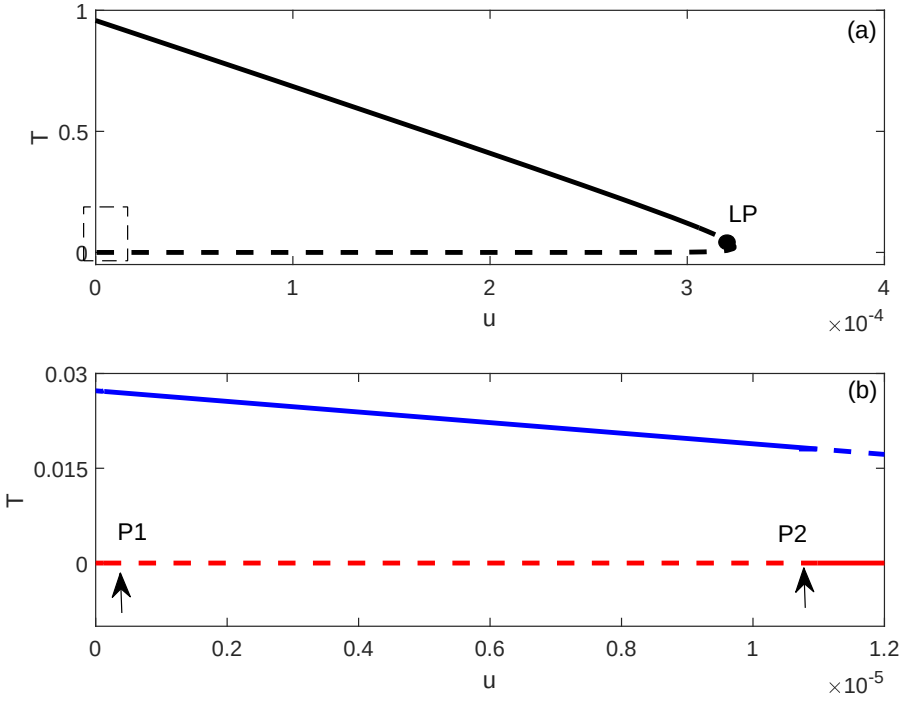

Figure 7. Bifurcation diagram for the model with chemotherapy for the system parameters in Table 1 with ($\delta = 0.0005$, $\nu = 0.97$) and drug intensity u as the main bifurcation parameter. Solid line (stable branch); dashed line (unstable branch); LP (static limit point); (**a**) Diagram with high-tumor steady state only; (**b**) free-tumor equilibrium (red); and low-tumor equilibrium (blue); (P_1) and (P_2) are critical points. The dotted box in Figure 7a is enlarged in Figure 7b.

Since the location of the critical points P_1 and P_2 is governed by the simple quadratic equation (Equation (11)), it is straightforward to examine the effect of model parameters on the location of these points and therefore on the range of the instability region between them. Figure 8 shows the effect of the model parameters in a qualitative way, where Δ denotes the range (in terms of u between P_1 and P_2). We recall that γ is the rate of tumor cell lysis, ν the saturation level of fractional tumor cell kill law, and δ the rate of the natural death of effector cells. The chemotherapy parameters are μ (the rate of change in the chemotherapy drug over time), and k_1 and k_2 are the killing effects of chemotherapy on the tumor and effector cells, respectively.

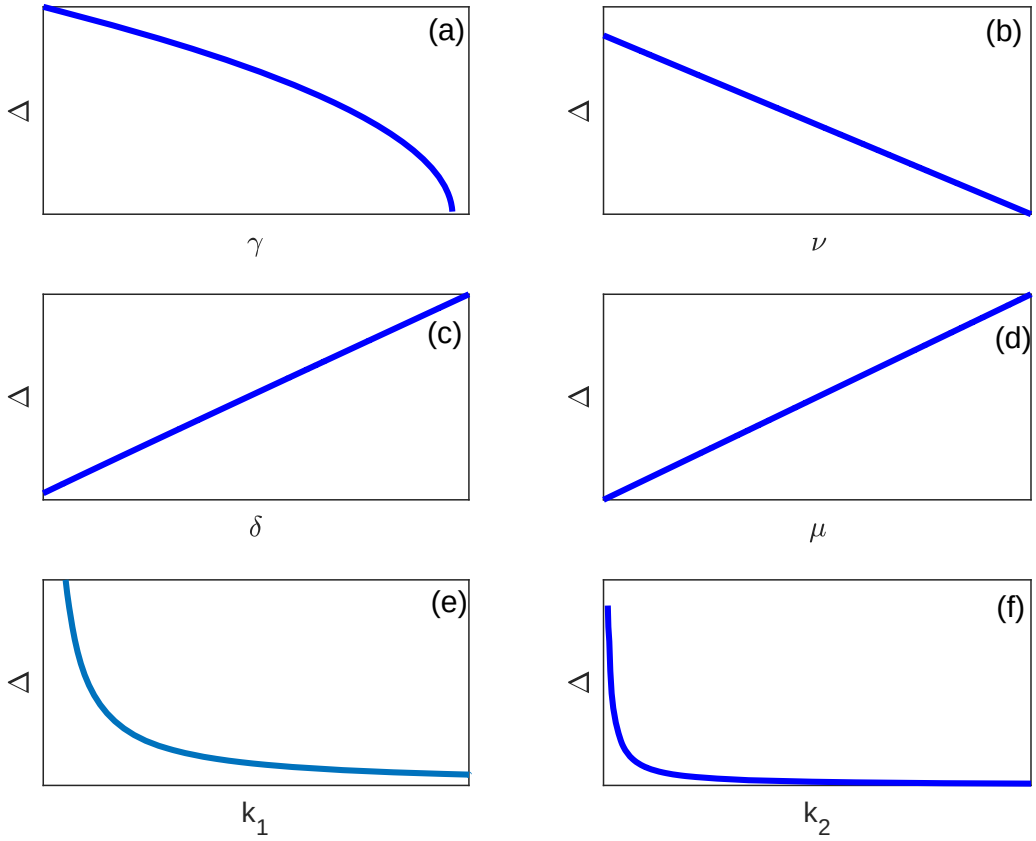

Figure 8. Effect of model parameters on the range (Δ) of the instability region (between P_1 and P_2 of Figure 7b). (**a**) Effect of rate of tumor cell lysis γ; (**b**) effect of saturation level of fractional tumor cell killing ν; (**c**) effect of death rate of effector cells δ; (**d**) effect of rate of chemotherapy drug decay μ; (**e**) effect of fractional tumor cell killing by chemotherapy k_1; (**f**) effect of fractional immune cell killing by chemotherapy k_2.

It can be seen that as γ increases, the range of instability decreases until it disappears as both points P_1 and P_2 collapse into a single point. The same can be seen for the effect of ν. On the other hand, the increase in δ increases the range of the instability region.

For the chemotherapy-related parameters, the increase in μ increases the region of instability. However, for both k_1 and k_2, the regime of instability decreases with the increase in any of these two parameters.

The effect of model parameters on the locus of the limit point of Figure 5 is, on other hand, shown in Figures 9 and 10. It can be seen that ν and γ decrease almost linearly with u. This means that if the parameters ν or γ increase, then the amount of chemotherapy drugs needed to completely suppress the tumor (i.e., past the limit point) will also decrease linearly. The trend of j is also a decreasing one, but it is in a limited range of u. On the other hand, the effect of ϕ, s, and δ shows a fast and increasing trend with u. This implies that should any of these parameters increase, the amount of drugs needed to completely

suppress the tumor would have to be increased. Lastly, Figure 10 shows the effect of chemotherapy-related parameters on the location of the limit point. As expected, k_1 (tumor-associated) decreases with u, while k_2 (effector-associated) increases. This means that larger values of k_1 or smaller values of k_2 will decrease the amount of chemotherapy drug needed to eliminate the tumor. The effect of μ is, on other hand, a decreasing one. Increasing the rate of chemotherapy drug will obviously reduce the amount of drug needed to reach a stable tumor-free equilibrium. A summary of the different bifurcation behaviors obtained without and with chemotherapy is shown in Table 3.

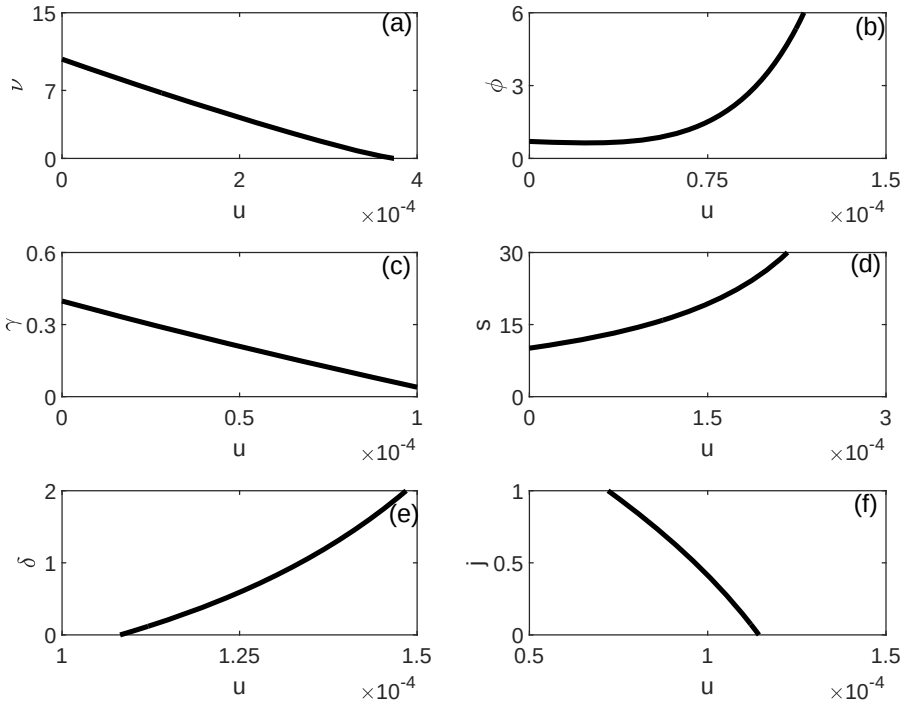

Figure 9. Two parameter continuation diagrams showing the effect of model biological parameters on the locus of the limit point of Figure 5. (**a**) Effect of saturation level of fractional tumor cell killing ν; (**b**) Effect of effector cell inactivation rate by tumor cells ϕ; (**c**) Effect of rate of tumor cell lysis γ; (**d**) Effect of steepness coefficient of the PRW law s; (**e**) Effect of death rate of effector cells δ; (**f**) Effect of maximum recruitment rate related to the power law j.

Table 3. Summary of bifurcation behaviors found in the different diagrams.

Figure 2	Key par. ($u = 0$)	Bif. par. (γ)	$[0, LP]$ TF,HT	$\geq LP$ TF		
Figure 3	Key par. ($\nu = 0.5$)	Bif. par. (γ)	$[0, P]$ HT	$[P, LP]$ TF,HT	$\geq LP$ TP	
Figure 5	Key par. ($\nu = 6.75$)	Bif. par. (u)	$[0, LP]$ TF,HT	$\geq LP$ TF		
Figure 6	Key par. ($\nu = 0.95$)	Bif. par. (u)	$[0, P]$ HT	$[P, LP]$ TF,HT	$\geq LP$ TF	
Figure 7a,b	Key par. ($\delta = 0.0005, \nu = 0.97$)	Bif. par. (u)	$[0, P_1]$ TF,HT	$[P_1, P_2]$ MT,HT	$[P_2, LP]$ TF,HT	$\geq LP$ TF

Bif. par.: Bifurcation parameter in the figure (x-axis). Key par.: All model parameter values are taken from Table 1, except the value of the key parameter associated with the figure. MT: Medium tumor levels. HT: High tumor levels. TF: Tumor-free equilibrium. $[-, -]$: Range of the bifurcation parameter. X,Y: The stable coexistence of equilibria X and Y.

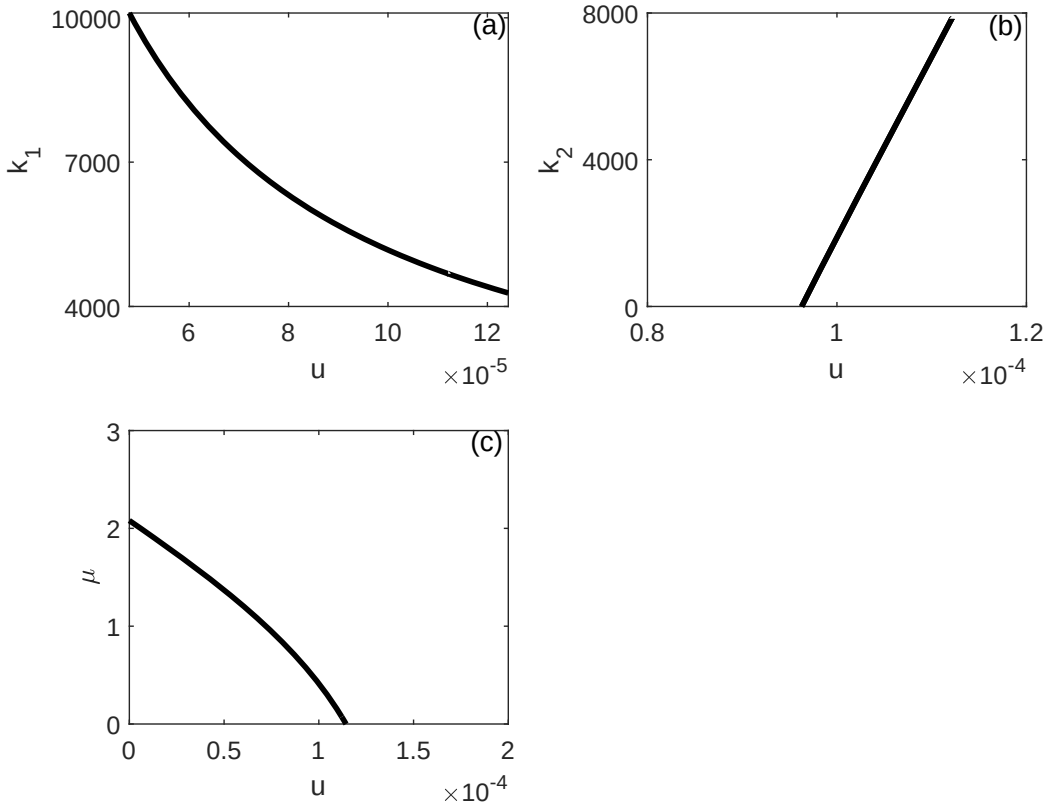

Figure 10. Two parameter continuation diagrams showing the effect of model chemotherapy-related parameters on the locus of the limit point of Figure 5. (**a**) Effect of fractional tumor cell killing by chemotherapy k_1; (**b**) Effect of fractional immune cell killing by chemotherapy k_2. (**c**) Effect of rate of chemotherapy drug decay μ.

7. Biological Interpretation

The goal of this work was to study a relatively simple model to encapsulate the expected behaviors of tumor–immune cell competition.

In the absence of immunotherapy or chemotherapy, the model was able to predict a saddle–node bifurcation for any small changes in model parameters. In reality, due to the non-uniformity of effector and tumor cell populations and the presence of distinct subpopulations characterized by unique parameter values that dictate their behavior, it is highly probable that variations in these parameter values will occur.

Depending on the values of the parameters, the outcome may manifest in one of three ways: an elimination scenario where immune cells proficiently eliminate cancer cells; a steady-state coexistence where the immune system exhibits reduced efficiency, containing the tumor without achieving its complete removal; or a situation in which the immune system fails to function effectively, resulting in uncontrolled tumor growth.

In the presence of bistability, where a high-tumor state exists alongside a tumor-free state, a treatment that directs the system towards the stable equilibrium of the tumor-free basin of attraction may result in a healthy condition. For instance, adaptive cell transfer may be employed to enhance the quantity of immune cells, while radiation or surgical interventions can be utilized to reduce the tumor population [15].

For other parameter space, the equilibrium without tumors is unstable, and merely reducing the tumor size is insufficient. In order to achieve a stable equilibrium, any treatment approach aimed at effectively eliminating a tumor must not only decrease the tumor load but also alter the system's parameters [10]. Thus, immunotherapy may be perceived as a treatment that changes systemic conditions, including the long-lasting enhancement of immune cells' cytolytic capabilities.

In the presence of chemotherapy treatment, the situation is more complex. The model predicted three different situations that depend exclusively on the relative importance of the system biological parameters γ, δ and ν and the chemotherapy parameters k_1 and k_2 in addition to the level of administrated drug u. We recall that γ is the rate of tumor cell lysis, δ the rate of natural demise of effector cells, and ν the saturation level of fractional tumor cell killing law.

If ν is larger than unity, then the tumor-free equilibrium is always stable for any values of the other model parameters, or any level of administrated drug. Bistability between tumor-free and high-tumor cells also prevails in this case, and only values of u larger than the saddle–node critical point will completely suppress the tumor. This critical value of the drug can be lowered by attempting to increase ν,γ or decrease ϕ, s or δ.

If $\nu < 1$, $\nu < 1 - \frac{\gamma}{\delta}$, and $\nu < 1 - \frac{\delta k_1}{k_2}$, then there is a critical value of u below which the tumor-free equilibrium is unstable. This means that values of drug u smaller than the critical value can not stop the growth of the tumor. Beyond that, there is bistability, and depending on the rates $\frac{k_1}{k_2}$, the basin of attractions can be altered.

If ν is such that $1 - \frac{\gamma}{\delta} < \nu < 1 - \frac{\delta k_1}{k_2}$, then the disease-free equilibrium is unstable between the two critical values of the drug intensity u. Moreover, there is the appearance of a non-trivial middle tumor concentration equilibrium. That means that relatively large doses of chemotherapy (between the two critical points) are not able to suppress the tumor but rather cause the existence of bistabiity between a low-level tumor cell and high-tumor cell steady states. This interesting scenario illustrates the unexpected results that may arise from the intricate interactions between the biological parameters of the model and its chemotherapy parameters.

The middle steady-state may represent a chronic controlled tumor burden, where the immune system is active but not completely successful in eliminating the tumor or the tumor persists without unchecked growth, similar to what is seen in cancer dormancy. This might resemble clinical remission or indolent tumors that are not progressing but also are not fully eradicated. The existence of dormant cancer cells in many common cancers has been clinically documented in cases where organ transplant recipients developed cancers originating from dormant tumor cells present in donor organs [35]. These cases highlight how immunosuppression can awaken previously dormant tumor cells [35]. Other studies have shown that the immune system plays a crucial role in maintaining tumor dormancy [36].

8. Conclusions

This study analyzed the dynamic interactions between tumor cells and immune effector cells without and with chemotherapy. The model incorporated a Hill function to describe the fractional cell kill law and the logistic growth for tumor cells, while simplifying the immune response by linearly combining the dynamics of NK and CTL cells into a single effector cell population. The analysis focused on the stability of equilibrium points and the identification of bistability regimes, which are critical for understanding tumor progression and treatment outcomes. The findings of this analysis provided some insights for optimizing cancer treatment strategies, particularly in the context of chemotherapy and immune system interactions. Below are the key clinical implications.

1. Personalized treatment based on immune parameters:
    - The model highlighted that the effectiveness of chemotherapy depends on the patient's immune parameters (e.g., γ, δ, ν).
    - Patients with a strong innate immune response ($\nu > 1$) may require lower chemotherapy doses to achieve tumor suppression, reducing toxicity risks. Conversely, patients with weaker immune responses ($\nu < 1$) may need higher drug

doses or additional immunotherapy to shift the system toward a tumor-free equilibrium.

2. Importance of bistability in treatment:
    - The presence of bistability (coexistence of tumor-free and high-tumor states) suggests that small changes in immune function or tumor burden can drastically alter outcomes.
    - Immunostimulatory therapies (e.g., checkpoint inhibitors, adoptive T-cell transfer) could help push the system into the tumor-free basin of attraction.
3. Optimizing chemotherapy dosing:
    - The model identified critical drug thresholds where chemotherapy either succeeds or fails. Below a certain dose, the tumor may persist or even grow (treatment resistance). Above the threshold, complete tumor suppression is possible.
    - Combination therapies (chemotherapy and immunotherapy) may help lower the required drug dose while improving outcomes.
4. Unintended effects of chemotherapy:
    - High chemotherapy doses can deplete effector cells (k_2 effect), weakening immune surveillance and potentially leading to relapse.
    - The model suggests that balancing k_1 (tumor kill rate) and k_2 (immune cell kill rate) is crucial. Drugs with high tumor specificity ($k_1 >> k_2$) are preferable.
5. Predictive biomarkers for treatment response:
    - Parameters like γ (immune cell killing efficiency) and ν (saturation of immune response) could serve as biomarkers with which to predict which patients will respond to chemotherapy.
    - Patients with low γ or ν may benefit from adjuvant immunotherapy to enhance immune-mediated tumor killing.
6. Potential for adaptive therapy:
    - Since the model showed parameter-dependent thresholds, adaptive therapy (adjusting drug doses based on tumor–immune dynamics) could improve outcomes while minimizing side effects.
    - Monitoring immune cell levels during treatment could help guide dose adjustments in real time.

Future clinical studies could validate these predictions by correlating immune parameters (γ, ν, δ) with patient outcomes, paving the way for more precise and effective cancer treatments.

Other future directions of the work could include the following. The model assumed constant drug administration. Incorporating pharmacokinetics/dynamics (e.g., drug clearance, intermittent dosing) could improve realism. It might also be worth exploring the model with immune response delay. Time delays are important, because immune responses do not occur instantaneously as they involve multi-step biological processes with inherent lags. Adjusting time delay could also yield richer dynamics [37].

Author Contributions: Conceptualization, A.A. and R.T.A.; methodology, A.A., R.T.A. and E.H.A.; software, A.A. and R.T.A.; validation, A.A. and R.T.A.; formal analysis, A.A., R.T.A. and E.H.A.; resources R.T.A. and E.H.A.; writing—original draft preparation, A.A. and R.T.A.; project administration, R.T.A. and E.H.A.; funding acquisition, R.T.A. All authors have read and agreed to the published version of the manuscript.

Funding: This work was supported and funded by the Deanship of Scientific Research at Imam Mohammad Ibn Saud Islamic University (IMSIU) (grant number IMSIU-DDRSP2501).

Data Availability Statement: The original contributions presented in the study are included in the article. Further inquires can be directed to the corresponding author.

Conflicts of Interest: The authors declare no conflicts of interest. The funders had no role in the design of the study; in the collection, analyses, or interpretation of data; in the writing of the manuscript; or in the decision to publish the results.

Appendix A. Derivation of Non-Trivial Steady States and Study of Their Stability

The steady state of Equation (7) yields

$$C = \frac{u}{\mu}. \tag{A1}$$

Eliminating D from the steady sate form of Equation (5) and substituting it in Equation (8) yields

$$\bar{D} = \frac{\bar{E}^{\tau}}{\bar{s}\bar{T}^{\tau} + \bar{E}^{\tau}} = \frac{1 - \gamma E - k_1 C - T}{\nu} \tag{A2}$$

This yields a transcendental equation as function of E and T,

$$E^{\tau}(\nu - 1 + k_1 C + T) + \gamma E^{n+1} = sT^{n}(1 - \gamma E - k_1 C) - T^{\tau+1}, \tag{A3}$$

that can also be written as

$$lnE^{\tau} - ln(sT^{\tau} + E^{\tau}) = \frac{1 - \gamma E - k_1 CT}{\nu}. \tag{A4}$$

A second equation involving E and T can be obtained by substituting Equation (8) in Equation (6) to yield

$$a_3 E^3 + a_2 E^2 + a_1 E + a_0 = 0, \tag{A5}$$

where the coefficients $a_i, i = 1, 3$ depend explicitly on T.

$$a_0 = (k + T^2)(h\nu^2 + T^2(-1 + Ck_1 + T)^2). \tag{A6}$$

$$\begin{aligned} a_1 = {} & -C^3 k_1^2 k_2 T^2 (k + T^2) - \delta(k + T^2)(h\nu^2 + T^2(-1 + Ck_1 + T)^2) + C^2 k_1 T^2 (gk_1(k + T^2) - \\ & 2k_2(-1 + T)(k + T^2) - k_1 T(-jT + \phi(k + T^2))) + T(-h\nu^2(-jT + \phi(k + T^2)) + \\ & (-1 + T)T(2\gamma(k + T^2) + (-1 + T)(gk - k\phi T + (g + j)T^2 - \phi T^3))) - C(hk_2\nu^2(k + T^2) + \\ & T^2(-2\gamma k_1(k + T^2) + (-1 + T)(-2gk_1(k + T^2) + k_2(-1 + T)(k + T^2) + 2k_1 T(-jT + \phi(k + T^2))))), \end{aligned} \tag{A7}$$

$$a_3 = -\delta\gamma^2 kT^2 + \gamma^2 gkT^2 - C\gamma^2 k_2 kT^2 - \gamma^2 k\phi T^3 - \delta\gamma^2 T^4 + \gamma^2 gT^4 + \gamma^2 jT^4 - C\gamma^2 k_2 T^4 - \gamma^2 \phi T^5, \tag{A8}$$

$$\begin{aligned} a_2 = {} & \gamma T^2(\gamma(k + T^2) - 2\delta(-1 + Ck_1 + T)(k + T^2) - 2(-1 + Ck_1 + T)(-gk + Ck_2 k + \\ & k\phi T - (g + j - Ck_2)T^2 + \phi T^3)). \end{aligned} \tag{A9}$$

Given that a_0 is always positive, for a real and positive solution T, Equation (A5) is a polynomial of third order in E. The application of Descartes rule of sign stipulates that the maximum real and positive roots for Equation (A5) is three which corresponds to the case when $a_1 < 0$, $a_2 > 0$ and $a_3 < 0$.

For the local stability of the nontrivial steady state, the Jacobian matrix of the model (Equations (5)–(8)) is given by:

$$J = \begin{pmatrix} J_{1T} & J_{1E} & J_{1C} \\ J_{2T} & J_{2E} & J_{2C} \\ J_{3T} & J_{3E} & J_{3C} \end{pmatrix}. \tag{A10}$$

$$J_{1T} = 1 - \gamma E - k_1 C - 2T + \frac{s\tau\nu E^\tau T^\tau}{(E^\tau + sT^\tau)^2} - \frac{\nu E^\tau}{E^\tau + sT^\tau}$$

$$J_{1E} = -\gamma T + \frac{\tau\nu T E^{-1+2\tau}}{(E^\tau + sT^\tau)^2} - \frac{\tau\nu T E^{-1+\tau}}{E^\tau + sT^\tau}$$

$$J_{1C} = -k_1 T$$

$$J_{2T} = E(-\phi + \frac{2jkT}{(k+T^2)^2} - \frac{2(-1+\tau)gTE^{2\tau}}{2hsE^\tau T^\tau + hs^2T^{2\tau} + E^{2\tau}(h+T^2)} + \frac{2gE^{3\tau}T(s\tau hT^\tau + E^\lambda(\tau h + (-1+\tau)T^2))}{(2hsE^\tau T^\tau + hs^2T^{2\tau} + E^{2\tau}(h+T^2))^2})$$

$$J_{2E} = -\delta - k_2 C - \phi T + \frac{jT^2}{k+T^2} - \frac{2g\tau E^{3\tau}T^2}{(E^\tau+sT^\tau)^3(h+\frac{E^{2\tau}T^2}{(E^\tau+sT^\tau)^2})} + \frac{g(1+2\tau)E^{2\tau}T^2}{(E^\tau+sT^\tau)^2(h+\frac{E^{2\tau}T^2}{(E^\tau+sT^\tau)^2})} - \frac{gE^{1+2\tau}T^2(\frac{-2\tau E^{-1+3\tau}T^2}{(E^\tau+sT^\tau)^3} + \frac{2\tau E^{-1+2\tau}T^2}{(E^\tau+sT^\tau)^2})}{(E^\tau+sT^\tau)^2(h+\frac{E^{2\tau}T^2}{(E^\tau+sT^\tau)^2})^2}$$

$$J_{2C} = -k_2 E$$

$$J_{3T} = 0$$

$$J_{3E} = 0$$

$$J_{3C} = -\mu$$

Since $J_{3T} = 0$ and $J_{3E} = 0$, one eigenvalue is $\lambda = -\mu$, while the two other satisfy

$$\lambda^2 - (J_{1T} + J_{2E})\lambda + (J_{1T}J_{2E} - J_{1E}J_{2T}) = 0. \tag{A11}$$

The elements $(J_{1T} + j_{2E})$ and $(J_{1T}J_{2E} - J_{1E}J_{2T})$ are respectively the trace and determinant of the 2 by 2 Jacobian matrix formed by eliminating the third equation (Equation (7)) that does not depend on the two others. The local stability of the eigenvalues is based on the sign of trace and determinant although numerical analysis is essential because of the transcendental nature of the equations. The same can be said about the study of occurrence of saddle–node bifurcation using the Sotomayor theorem [38].

Appendix B. Derivation of Equations (11) and (12) for Eigenvalues of Tumor-Free Equilibrium

Substituting for the tumor-free conditions, $T = 0, E = \frac{1}{\delta + k_2 C}, C = \frac{u}{\mu}$ yields the following elements of the Jacobian matrix.

$$J_{1T} = 1 - \nu - \frac{k_1 u}{\mu} - \frac{\gamma}{\delta + \frac{k_2 u}{\mu}}$$

$$J_{1E} = 0, J_{1C} = 0$$

$$J_{2T} = \frac{-\phi}{\delta + \frac{k_2 u}{\mu}}$$

$$J_{2E} = -\delta - \frac{k_2 u}{\mu}$$

$$J_{2C} = \frac{-k_2}{\delta + \frac{k_2 u}{\mu}}$$

$$J_{3T} = 0; J_{3E} = 0; J_{3C} = -\mu.$$

The eigenvalues of the Jacobian matrix can be readily obtained and are those of Equations (11) and (12).

References

1. Bray, F.; Laversanne, M.; Sung, H.; Ferlay, J.; Siegel, R.L.; Soerjomataram, I.; Jemal, A. Global cancer statistics 2022: GLOBOCAN estimates of incidence and mortality worldwide for 36 cancers in 185 countries. *CA Cancer J. Clin.* **2024**, *74*, 229–263. [CrossRef] [PubMed]
2. Apavaloaei, A.; Hardy, M.-P.; Thibault, P.; Perreault, C. The origin and immune recognition of tumor-specific antigens. *Cancers* **2020**, *12*, 2607. [CrossRef]
3. Rosenberg, J.; Huang, J. CD8+ T Cells and NK Cells: Parallel and Complementary Soldiers of Immunotherapy. *Curr. Opin. Chem. Eng.* **2018**, *19*, 9–20. [CrossRef]
4. Chiossone, L.; Dumas, P.Y.; Vienne, M.; Vivier, E. Natural killer cells and other innate lymphoid cells in cancer. *Nat. Rev. Immunol.* **2018**, *18*, 671–688. [CrossRef]
5. Brummelman, J.; Mazza, E.M.; Alvisi, G.; Colombo, F.S.; Grilli, A.; Mikulak, J.; Mavilio, D.; Alloisio, M.; Ferrari, F.; Lopci, E.; et al. High dimensional single cell analysis identifies stem-like cytotoxic CD8+ T cells infiltrating human tumors. *J. Exp. Med.* **2018,** *215*, 2520–2535. [CrossRef] [PubMed]
6. Bellomo, N.; Li, N.K.; Maini, P.K. On the foundations of cancer modelling: Selected topics, speculations, and perspectives. *Math. Model. Methods Appl. Sci.* **2008**, *18*, 646. [CrossRef]
7. Brady, R.; Enderling, H. Mathematical models of cancer: When to predict novel therapies, and when not to. *Bull. Math. Biol.* **2019**, *81*, 3722. [CrossRef] [PubMed]
8. Kuznetsov, V.; Makalkin, I.; Taylor, M.; Perelson, A. Nonlinear dynamics of immunogenic tumors: Parameter estimation and global bifurcation analysis. *Bull Math Biol.* **1994**, *56*, 295–321. [CrossRef]
9. Pillis, L.G.D.; Radunskaya, A. The dynamics of an optimally controlled tumor model: A case study. *Mathl. Comput. Model.* **2003**, *37*, 221–1244. [CrossRef]
10. Pillis, L.G.D.; Radunskaya, A.E.; Wiseman, C.L. A validated mathematical model of cell mediated immune response to tumor growth. *Cancer Res.* **2005**, *65*, 7950–7958. [CrossRef]
11. de Pillis, L.G.; Radunskaya, A.E. *Modeling Tumor-Immune Dynamics, in Mathematical Models of Tumor-Immune System Dynamics*; Kim, A.E.P., Mallet, D., Eds.; Springer: Berlin/Heidelberg, Germany, 2014; pp. 59–108.
12. Mirzaei, N.M.; Tatarova, Z.; Hao, W.; Changiz, N.; Asadpoure, A.; Zervantonakis, I.K. A PDE model of breast tumor progression in MMTV-PyMT Mice. *J. Pers. Med.* **2022**, *12*, 807. [CrossRef] [PubMed]
13. López, A.G.; Seoane, J.M.; Sanjuán, M.A.F. A validated mathematical model of tumor growth including tumor-host interaction, cell-mediated immune response and chemotherapy. *Bull. Math. Biol.* **2014**, *76*, 2884–2906. [CrossRef]
14. Makhlouf, A.M.; El-Shennawy, L.; Elkaranshawy, H.A. Mathematical modelling for the role of CD4+T cells in tumor-immune interactions. *Comput. Math. Methods Med.* **2020**, *2020*, 7187602. [CrossRef] [PubMed]
15. Song, G.; Tian, T.; Zhang, X. A mathematical model of cell-mediated immune response to tumor. *Math. Biosci. Eng.* **2020**, *18*, 373–385. [CrossRef]
16. Rihan, F.A.; Rajivganthi, C. Dynamics of tumor-immune system with random noise. *Mathematics* **2021**, *9*, 2707. [CrossRef]
17. Bashkirtseva, I.; Chukhareva, A.; Ryashko, L. Modeling and analysis of nonlinear tumorimmune interaction under chemotherapy and radiotherapy. *Math. Meth. Appl. Sci.* **2022**, *45*, 7983–7991. [CrossRef]
18. Sardar, M.; Khajanchi, S.; Biswas, S. Stochastic dynamics of a nonlinear tumor-immune competitive system. *Nonlinear Dyn.* **2025**, *113*, 4395–4423. [CrossRef]
19. Sardar, M.; Biswas, S.; Khajanchi, S. Modeling the dynamics of mixed immunotherapy and chemotherapy for the treatment of immunogenic tumor. *Eur. Phys. J. Plus.* **2024**, *139*, 228. [CrossRef]
20. Kareva, I.; Luddy, K.A.; O'Farrelly, C.; Gatenby, R.A.; Brown, J.S. Predator-prey in tumor-immune interactions: A wrong model or just an incomplete one? *Front. Immunol.* **2021**, *12*, 668221. [CrossRef]
21. Diefenbach, A.; Jensen, E.R.; Jamieson, A.M.; Raulet, D.H. Rae1 and H60 ligands of the NKG2D receptor stimulate tumour immunity. *Nature* **2001**, *413*, 165–171. [CrossRef]
22. Dudley, M.E.; Wunderlich, J.R.; Robbins, P.F.; Yang, J.C.; Hwu, P.; Schwartzentruber, D.J.; Topalian, S.L.; Sherry, R.; Restifo, N.P.; Hubicki, A.M.; et al. Cancer regression and autoimmunity in patients after clonal repopulation with antitumor lymphocytes. *Science* **2002**, *298*, 850–854. [CrossRef] [PubMed]

23. Hill, A.V. The possible effects of the aggregation of the molecules of haemoglobin on its dissociation curves. *J. Physiol.* **1910**, *40*, 4–7.
24. Trapani, J.A.; Smyth, M.J. Functional significance of the perforin/granzyme cell death pathway. *Nat. Rev. Immunol.* **2002**, *2*, 735–747. [CrossRef]
25. Screpanti, V.; Wallin, R.P.; Grandien, A.; Ljunggren, H.G. Impact of FASL-induced apoptosis in the elimination of tumor cells by NK cells. *Mol. Immunol.* **2005**, *42*, 495–499. [CrossRef] [PubMed]
26. Waldhauer, I.; Steinle, A. NK cells and cancer immunosurveillance. *Oncogene* **2008**, *27*, 5932–5943. [CrossRef]
27. Galon, J.; Bruni, D. Approaches to treat immune hot, altered and cold tumours with combination immunotherapies. *Nat. Rev. Drug Discov.* **2019**, *18*, 197–218. [CrossRef]
28. Kirschner, D.; Panetta, J.C. Modeling immunotherapy of the tumor-immune interaction. *J. Math. Biol.* **1998**, *37*, 235–252. [CrossRef]
29. Eftimie, R.; Bramson, J.L.; Earn, D.J. Interactions between the immune system and cancer: A brief review of non-spatial mathematical models. *Bull. Math. Biol.* **2011**, *73*, 2–32. [CrossRef]
30. Dunn, G.P.; Old, L.J.; Schreiber, R.D. The immunobiology of cancer immunosurveillance and immunoediting. *Immunity* **2004**, *21*, 137–148. [CrossRef]
31. Wei, S.C.; Levine, J.H.; Cogdill, A.P.; Zhao, Y.; Anang, N.-A.A.S.; Andrews, M.C.; Sharma, P.; Wang, J.; Wargo, J.A.; Pe'Er, D.; et al. Distinct cellular mechanisms underlie anti-CTLA-4 and anti-PD-1 checkpoint blockade. *Cell* **2017**, *170*, 1120–1133.e17. [CrossRef]
32. Smyth, M.J.; Ngiow, S.F.; Ribas, A.; Teng, M.W. Combination cancer immunotherapies tailored to the tumour microenvironment. *Nat. Rev. Clin. Oncol.* **2016**, *13*, 143–158. [CrossRef] [PubMed]
33. Dhooge, A.; Govaerts, W.; Kuznetsov, Y.A.; Meijer, H.G.; Sautois, B. New features of the software MatCont for bifurcation analysis of dynamical systems. Version 7p6; *MCMDS* **2008**, *14*, 147–175.
34. *MATLAB Version: 9.13.0 (R2022b)*; The MathWorks Inc.: Natick, MA, USA, 2022.
35. Matser, Y.A.H.; Terpstra, M.L.; Nadalin, S.; Nossent, G.D.; de Boer, J.; van Bemmel, B.C.; van Eeden, S.; Budde, K.; Brakemeier, S.; Bemelman, F.J. Transmission of breast cancer by a single multiorgan donor to 4 transplant recipients. *Am. J. Transplant.* **2018**, *18*, 1810–1814. [CrossRef] [PubMed]
36. Phan, T.G.; Croucher, P.I. The dormant cancer cell life cycle. *Nat. Rev. Cancer.* **2020**, *20*, 398–411. [CrossRef]
37. Sardar, M.; Khajanchi, S.; Biswas, S.; Abdelwahab, F.S.; Nisar, K.S. Exploring the dynamics of a tumor-immune interplay with time delay. *Alex. Eng. J.* **2021**, *60*, 4875–4888. [CrossRef]
38. Sotomayor, J. Generic bifurcations of Ddynamical systems. In Proceedings of a Symposium Held at the University of Bahia, Salvador, Brazil, 26 July 26–14 August 1971; pp. 561–582. [CrossRef]